

Coated Dielectric Lens Design, Modelling and Measurements for Future CMB Polarimetry Missions

P. C. Hargrave¹, G. Savini², N. Trappe³, A. Challinor^{4,5}, S.B. Sørensen⁶, P. A. R. Ade¹, R. V. Sudiwala¹, I. K. Walker¹, M. Gradziel³, N. Tynan³, M. van der Vorst⁷

¹ School of Physics & Astronomy, Cardiff University, Cardiff, UK

² Optical Science Laboratory, Physics & Astronomy Dep., University College London, London, UK

³ National University of Ireland, Maynooth, Ireland

⁴ Institute of Astronomy and Kavli Institute for Cosmology Cambridge, Madingley Road, Cambridge, CB3 0HA, UK

⁵ DAMTP, Centre for Mathematical Sciences, Wilberforce Road, Cambridge, CB3 0WA, UK

⁶ TICRA, Copenhagen, Denmark

⁷ European Space Agency Antenna and Submillimetre Wave Section, ESTEC, The Netherlands

Abstract—We present an ongoing programme of work to investigate the use of large dielectric lenses with coating layers for future satellite-based cosmic microwave background (CMB) polarimetry missions. The primary purpose of this study is to validate modelling and manufacturing techniques. We present details of the study, and preliminary results of material and lens testing.

Index Terms—astronomy, dielectric, lens, telescope, modelling, measurements, polarimetry, satellite

I. INTRODUCTION

The detection of the curl-like B-mode polarization of the cosmic microwave background (CMB) induced by a stochastic background of primordial gravitational waves is well recognized as a key test of cosmic inflation in the early universe. Future satellite instruments have been proposed [1, 2] to measure this signal down to the limit set by confusion from gravitational lensing. This requires the use of an optical system with exquisite control over polarization systematics. In this paper we present the findings of an on-going ESA-funded study for an all-refractive telescope system to meet these very demanding scientific requirements. The baseline design solution comprises three dielectric lenses per telescope barrel, with a separate telescope barrel for each of the five frequency bands. All lenses will be anti-reflection coated, and are required to operate below 70 K. There is much uncertainty over the optical performance of dielectric lenses, particularly at low temperatures, and particularly in regard to polarization effects. We present the key results of the modelling and test programme for this study.

II. SCIENCE REQUIREMENTS

A detailed derivation of the science requirements is beyond the scope of this paper [3-5], but we report here simply the top-level requirements on the optical system that drove the design. The goal of the mission is to measure the B-mode power from primordial gravitational waves to the limit set by confusion from gravitational lensing. For multipoles $l < 200$, the latter has a white-noise spectrum $C_l^B \sim 1.7 \times$

$10^{-6} \mu K^2$ corresponding to uncorrelated polarization noise with $\Delta_P \sim 4.5 \mu K$ arcmin. The level of instrument noise in the polarization maps after foreground cleaning should therefore be better than $\Delta_P \sim 5 \mu K$ arcmin. In practice, a noise level of around $3 \mu K$ arcmin should be achievable after foreground cleaning over at least 50% of the sky (and rather more with prior information on the angular uniformity of the spectral behaviour of the foregrounds). This translates into a requirement on the number of detectors required to meet this sensitivity for a set mission duration [3]. The baseline design assumes feedhorn-coupled detectors, and hence the focal plane must be large enough to accommodate all detectors (two detectors per feedhorn, orthogonal polarizations).

The amplitude of the B-mode signal generated during inflation is expected to decay rapidly at small angular scales, so in principle high angular resolution is not required for a detection of B-modes. Therefore the angular resolution requirements are not very demanding, being from $10'$ to $50'$ respectively over the frequency range from 70 to 353 GHz.

We selected five bands which would allow us to achieve the mission sensitivity goals of $3 \mu K$ in 30% spectral bands at 70, 100, 143, 217 GHz, and $10 \mu K$ at 353 GHz.

Exquisite control of systematic effects is crucial for B-mode polarimetry, and we require excellent knowledge of the systematic effects induced by the optical system itself. It is very important to minimize instrumental polarization (leakage from temperature signal into the much weaker polarization). We set a specification on integrated cross-polar levels better than -30 dB [3, 5].

III. TELESCOPE BASELINE DESIGN

A. Choice of feed

The baseline feed choice is the use of ultra-Gaussian horns, as designed for the CLOVER experiment [6, 7]. The ultra-Gaussian horn design deliberately excites HE₁₂ higher order modes in a sine-square profile section of the horn, followed by an extended parallel section designed to bring

the HE12 mode into phase with the dominate HE11 mode. Wide bandwidths at the 30% level, with sidelobes well below -35dB are achieved. The feed horns exhibit very low cross-polarization content and low beam pattern ellipticity ($< 2\%$) for the best possible match with the Airy disc produced by the optical system at the focal surface position.

B. Telescope baseline design

Reflective, refractive or hybrid solutions could all potentially achieve the required performance figures, but volume and mass restrictions for a small/medium mission such as B-Pol [2] allow only a few possible configurations.

For reflective optics the optimal geometry is the so-called Compact Range Antenna (CRA), or crossed Dragone optics [8, 9] which satisfies the Dragone-Mizuguchi condition for low cross polarization and also has small aberrations across a large focal plane. Furthermore, the CRA telescopes have approximately flat focal surfaces and, suitably configured, are almost image-space telecentric.

Refractive optical configurations can be rotationally symmetric and thus very compact, and with relatively small scan aberrations and cross-polarization. But there are many uncertainties regarding the performance related to the lens material, electromagnetic and cryogenic properties, and modelling of such systems. The theoretical performance of the refracting telescopes is high and they have several advantages over reflecting telescopes. The most obvious advantage arises because the number and spacing of the surfaces, and the materials from which the lenses are to be produced, allow for the use of appropriate conic surfaces giving better control of aberration than would be possible in any compact two mirror telescope. This leads to beams of low ellipticity across the full focal array.

A full system trade-off for a future satellite mission was carried out, which took into account such factors as optical performance, mass, volume, cost, technology readiness and modelling capability. The result was marginal between an all-reflective system, and an all-refractive system. An all-refractive system was chosen for further study, as there would be more to be gained from a technology-development perspective.

The requirements for B-Pol [2] demand a wide field of view which is characteristic of camera lenses, not of classical telescopes. At the same time very low beam distortion is essential because of the stringent ellipticity requirements. To meet the field and performance requirements with the number of pixels set as goals, an optical configuration based upon a Petzval camera lens has been chosen. Classically such lenses comprise two positive doublets and, in the attempt to flatten the field, negative field flattener. A field flattener cannot be used for B-Pol because it would lead to acute beam angles at the horn array, but if a spherical focal surface of very large radius is accepted, then a modification of the Petzval lens will give high performance optical systems meeting almost all of the goals with a minimum of complexity. The general layout is illustrated in Figure 1. In this design, the chosen lens material is ultra-high molecular weight polyethylene (UHMW-PE), with an assumed

refractive index of 1.523 at all frequencies (see section IV). The theoretical semi-field of view spans 9.5° from the telescope axis, which at the focal surface translates into an available circular area of 165 mm radius for placement of the horns.

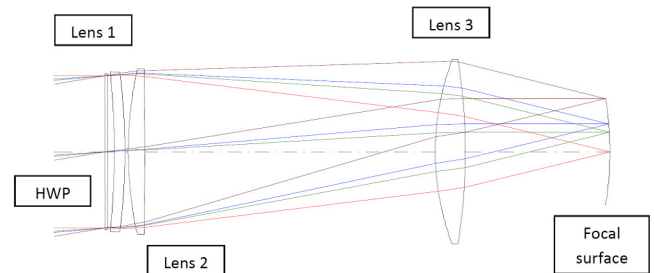


Figure 1. Refractive system based on the Petzval camera design. HWP denotes the nominal position of a half-wave plate, should one be required.

Because of the wide frequency coverage, and the large number of detectors that need to be accommodated on the focal plane, the payload is divided into multiple telescope/focal plane systems, each optimized to a particular frequency band. This approach also allows us to optimize the anti-reflection coating to each band. The telescope design is described in detail in *Hargrave et al.* [10] and *Candotti et al.* [5].

IV. LENS DEVELOPMENT DESIGN AND MANUFACTURING

There are many uncertainties over the use of refractive elements in this frequency range, such as;

- knowledge of the refractive index as a function of frequency and temperature,
- uniformity of the material,
- polarization effects in the material (e.g. stress-induced bi-refringence),
- uniformity and performance of any applied matching layer.

A modelling and test programme has been implemented to address these uncertainties, and to validate software models for future instrument design. We describe this modelling and test programme in the following sections.

A. Modelling

The requirements on the accuracy of the analysis tools are very challenging. The lenses are electrically large and high accuracy is needed for the beam shapes and cross-polarization. The analysis must accurately take into account the effects of multiple reflections, coating layers and edge diffractions for both on-axis and off-axis feeds.

It appeared that none of the currently available tools were suitable for the task such that new software development was necessary. The software package GRASP from TICRA was updated with BoR-MoM (Body of Revolution Method of Moments) and PO (Physical Optics) modules for analysis of dielectric lenses with coating.

The BoR-MoM approach is in principle exact, but in the implementation of the method it is very important to represent the curved lens surface and equivalent electric and

magnetic currents accurately. We have therefore used curved surface segments (instead of linear segments) and higher order polynomial basis functions for representing the currents. Also the coating layers are treated accurately with separate current sheets on each interface between layers.

Although the BoR-MoM is an attractive approach, it requires much computation time, especially for coatings and off-axis sources. On the contrary the PO is very fast, but relies on certain high frequency approximations. It was found that if internal reflections inside the lens (and between lenses for multi-lens systems) are taken into account in the PO, very good agreement between PO and BoR-MoM is obtained. Also the coating layers can be treated accurately with PO by replacing the standard Fresnel refraction with plane wave refraction through multiple planar interfaces. As opposed to the BoR-MoM an off-axis source does not increase the computation time.

The selected approach has thus been to use the BoR-MoM to validate the PO in a number of representative cases and hereafter apply the much faster PO.

B. Material measurements

A significant component of this activity was a study of the materials involved in order to validate their optical performance to a high degree of accuracy [11, 12]. For this reason UHMW-PE (lens material), and porous PTFE (used as the anti-reflection coating material) were subject to rigorous optical analyses to determine their real and imaginary refractive index as a function of frequency and temperature. We show that accurate determination of these optical constants is paramount in order to predict the optical performance of the overall optical system. Additional tests for stress-induced bi-refringence were also performed in order to place an upper-limit on possible systematic effects which might occur due to un-planned stresses in the instrument cooldown.

C. Lens manufacturing

Two lens types (A and B) have been designed and built, using the *measured* refractive index for the same material batch for the lens design. This is very important to do, as significant variation in index has been seen for plastics of different origin. These have been CNC machined by a specialist plastics machining firm, and have been mechanically verified using a 3-dimensional coordinate measurement machine. They both have convex hyperbolic surfaces, but the first lens refocuses the incident field at the same distance (Figure 2), whereas the other lens transforms rays from a point source into a planar wavefront (Figure 3).

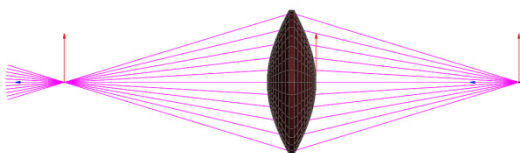


Figure 2. Schematic of Lens type-A

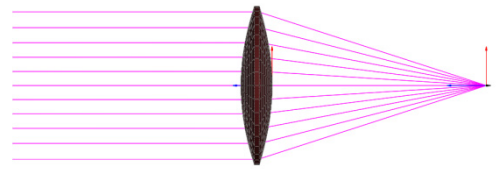


Figure 3. Schematic of Lens type-B

D. Anti-reflection coating

For a slab of dielectric material of index of refraction n_s , without AR coatings the reflective loss is given by

$$R = \left[\frac{(1 - n_s)}{(1 + n_s)} \right]^2$$

at each surface at normal incidence. The application of anti-reflection coating on a flat slab of dielectric substrate, with a given index of refraction n_s follows two very simple guidelines. The first is to ensure that a coating material with an optical index of refraction n_c is available, where $n_c = \sqrt{n_s}$ at the same frequency at which n_s is measured.

The second requirement is to make sure that it is possible to obtain, manufacture or engineer the thickness of the coating material such that its resulting thickness is one quarter of the required transmission wavelength within the material. For these lenses, we choose sheets of Porous-PTFE as the coating layer, bonded to the lens substrate using thin (few microns) sheets of low-density polyethylene. Both lens types will be anti-reflection coated, following an evolution of an existing process [13].

E. Lens measurements

Both lenses have a diameter of 286 mm and are being tested in the frequency range from 75 to 150 GHz. All tests will be carried out on the lenses in both their un-coated and coated states.

A high quality corrugated horn is used as a source, and a planar near-field x-y scanner probes the field at the opposite side of the lens. The double-convex hyperbolic lens (type-A, Figure 2) is tested to check its imaging properties with a 150GHz Gunn diode source and an incoherent detector which is scanned on the x-y plane orthogonal to the optical axis. This is repeated for a number of de-focus positions. The same test will also be performed off-axis with the source angled at 5-10°. Such a set of tests will allow us to assess to what degree of precision (and signal/noise) the lens performance matches the model prediction. Secondly, the same test set repeated after the lens coating procedure will verify the success of the coating procedure within the parameters required and how this affects the optical performance of the lens. The beam patterns of the source and probe horns are measured and characterized, and included in the analysis.

A spectral efficiency test was performed on lens type-A by direct re-imaging of a broadband source modulated with a polarizing Fourier Transform Spectrometer. This will also be

performed post-coating to verify if the coating is indeed performing as expected and validating how the converging beam modelling of the coating efficiency deviates from the nominal coating calculation for a flat element.

The type-B lens is undergoing a measurement campaign at W Band frequencies (75-110 GHz) using a vector network analyzer to measure both phase and amplitude in the near field (Figure 3), where a beam from the focus is transformed to a output beam with a flat phase front. The lens, when illuminated with a low edge taper beam by a corrugated horn placed at the focus of the lens, was scanned on the output side to measure the near field in a planar scan in both amplitude and phase. The setup is illustrated in Figure 4, with a corrugated source horn and a waveguide probe to measure the scanned output field. A rigorous alignment procedure was followed to ensure the source horn, lens and scan plane were all known. As the phase and amplitude information is conserved, a Gaussian field fitting programme was used to match the output beam profile to that of a reference Gaussian beam in order to characterize the beam in terms of centre position and outset angles in the horizontal and vertical axes. The lens was mounted on a rotation stage to allow illumination at different off-axis angles in the range 0 to 15°. The source horn was also moved along the propagation axis to vary to the output phase front of the beam. The scan plane was found to be not perfectly aligned perpendicular to the optical axis (source beam). Some misalignment can be tolerated here, but with the fitting routine used in the analysis, the small angular and offset misalignments are well known and may be included in the analysis and simulations.

This initial set of measurements was carried out on an uncoated lens and it is planned to repeat the measurements once the lens is coated. A preliminary measurement of the output beam at 100GHz with normal illumination of the lens is illustrated in Figure 5 in amplitude (dB) and phase (degrees).

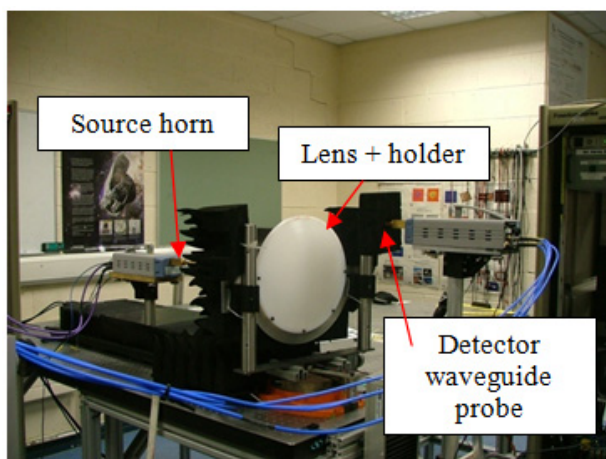


Figure 4. Optical bench holding source, detector and lens on rotation stage, to tilt lens relative to optical axis.

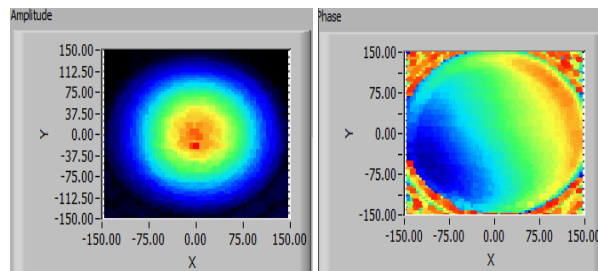


Figure 5. Amplitude and phase measurements at 100GHz with the lens in nominal position. The amplitude pattern is very symmetric but some residual stand wave artifacts are present. The phase curvature is extremely flat and has an equivalent radius of 34m

V. ANALYSIS

Comparison between the different analysis methods is given in this section. At the time of writing, only preliminary measured data was available. The test data will provide the ultimate software verification.

In Figure 2, the type-A lens is shown with the radiating horn to the right and the image focal point to the left. Analysis of this configuration with BoR-MoM and PO is shown in Figure 6. The field is computed through the focal point in the 45° plane, i.e. the bisector between the E- and H-plane to obtain maximum cross-polar field. It is seen that the agreement is very good even down to low levels. The 2nd order internal reflection included in PO is necessary to obtain this good agreement with the BoR-MoM which includes multiple reflections of all orders.

In Figure 3, the type-B lens is shown. Again the radiating horn is placed to the right and the refracted field with planar phase front is obtained to the left. The field is computed in the 45° cut as shown in Figure 7. In this case the phase of the field is shown since it is of primary interest whereas the amplitude will just resemble the feed pattern. Again an excellent agreement is obtained between BoR-MoM and PO.

In order to illustrate aberrations for off-axis feed positions the type-B lens is tilted 10° resulting in a distorted phase as shown in Figure 8. Measurements of such tilted lens configurations will also be carried out to provide detailed software validation.

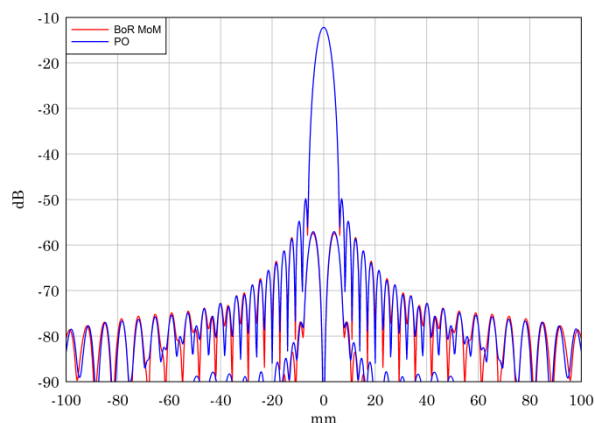


Figure 6 Type A lens. Comparison of analysis with BoR-MoM and PO.

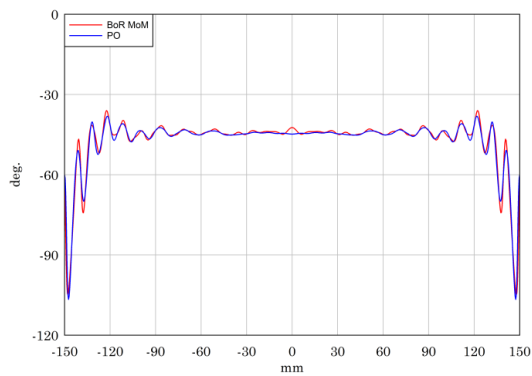


Figure 7 Type B lens. Comparison of analysis with BoR-MoM and PO.

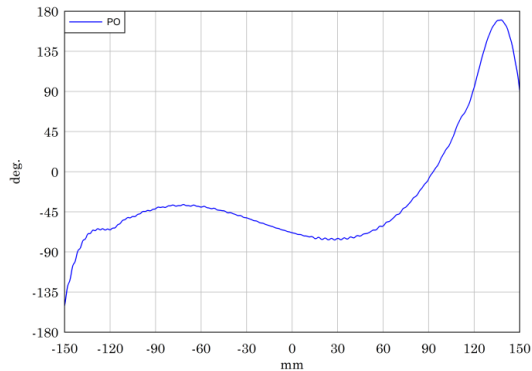


Figure 8 Type-A lens. Phase aberrations for 10° lens tilt.

VI. CONCLUSIONS

We have presented a summary of a comprehensive test programme designed to enable the consideration of refractive components in the design of future CMB polarimetry missions. This requires understanding of systematic effects to an unprecedented level of precision. This is particularly important, as several ground-based experiments already incorporate refractive elements [14-17]

ACKNOWLEDGEMENT

This work has been funded by the European Space Agency under contract number 4000102522/10/NL/AF2011.

REFERENCES

1. Armitage-Caplan, C., et al., *COrE (Cosmic Origins Explorer) A White Paper*. arXiv preprint arXiv:1102.2181, 2011.
2. Bernardis, P., et al., *B-Pol: detecting primordial gravitational waves generated during inflation*. *Experimental Astronomy*, 2009. **23**(1): p. 5-16.
3. Hargrave, P., A.D. Challinor, and T. Peacocke, *Review and consolidation of telescope instrument requirements (TN1)*, in *Modular Wide Field of View RF Configurations - ESTEC contract number 4000102522/10/NL/AF2011*, Cardiff University.
4. Hargrave, P., et al., *Telescope configuration trade-off report (TN2)*, in *Modular Wide Field of View*

5. Candotti, M., et al., *Mm and sub-mm Complete Refractive Telescope Electromagnetic Design for High Purity Electromagnetic Wave Polarization Detection*, in *ESA Workshop on large deployable antennas2012*, ESA: ESTEC.
6. Ade, P., R. Wylde, and J. Zhang. *Ultra-Gaussian Horns for CLOVER—a B-Mode CMB Experiment*. in *Twentieth International Symposium on Space Terahertz Technology*, edited by: E. Bryerton, A. Kerr, and A. Lichtenberger, Charlottesville. 2009.
7. North, C., et al. *Clover-Measuring the CMB B-mode polarization*. in *Eighteenth International Symposium on Space Terahertz Technology*. 2007.
8. Dragone, C., *Offset multireflector antennas with perfect pattern symmetry and polarization discrimination*. *AT T Technical Journal*, 1978. **57**: p. 2663-2684.
9. Dragone, C., *Unique reflector arrangement with very wide field of view for multibeam antennas*. *Electronics Letters*, 1983. **19**(25): p. 1061-1062.
10. Hargrave, P., et al., *Telescope baseline design report (TN3)*, in *Modular Wide Field of View RF Configurations - ESTEC contract number 4000102522/10/NL/AF2012*, Cardiff University.
11. Hargrave, P. and G. Savini, *Critical components and technologies identification (TN4)*, in *Modular Wide Field of View RF Configurations - ESTEC contract number 4000102522/10/NL/AF2012*, Cardiff University.
12. Hargrave, P. and G. Savini, *Critical Breadboards Definition and Analysis (TN5)*, in *Modular Wide Field of View RF Configurations - ESTEC contract number 4000102522/10/NL/AF2012*, Cardiff University.
13. Hargrave, P.C. and G. Savini. *Anti-reflection coating of large-format lenses for sub-mm applications*. in *SPIE Astronomical Telescopes and Instrumentation: Observational Frontiers of Astronomy for the New Decade*. 2010. International Society for Optics and Photonics.
14. Grainger, W., et al. *EBEX-The E and B Experiment*. in *Proc. of SPIE Vol.* 2008.
15. Lee, A.T., et al. *POLARBEAR: Ultra - high Energy Physics with Measurements of CMB Polarization*. 2008.
16. Chiang, H., et al., *Measurement of cosmic microwave background polarization power spectra from two years of BICEP data*. *The Astrophysical Journal*, 2010. **711**: p. 1123.
17. Ogburn IV, R., et al. *The BICEP2 CMB polarization experiment*. in *SPIE Astronomical Telescopes and Instrumentation: Observational Frontiers of Astronomy for the New Decade*. 2010. International Society for Optics and Photonics.